J Mater Sci (2009) 44:1294–1301
DOI 10.1007/s10853-009-3275-4

Effect of additives on the structure characteristics, thermal stability, reducibility and catalytic activity of CeO_2–ZrO_2 solid solution for methane combustion

Xiaohong Wang · Guanzhong Lu · Yun Guo · Liangzhu Jiang · Yanglong Guo · Chunzhong Li

Received: 15 April 2008 / Accepted: 14 January 2009 / Published online: 7 February 2009

Abstract M_yO_x-modified CeO_2–ZrO_2 (M = Al, Ba, Cu, La, Nd, Pr, Si) solid solutions with the atomic ratio of Zr/Ce = 1 were prepared by the reverse microemulsion method, and the effect of different additives on the structure characteristics, thermal stability, reducibility, and catalytic activity of CeO_2–ZrO_2 solid solution for methane combustion were investigated. According to their different effects, M_yO_x can be classified into three groups. The first group includes SiO_2 and Al_2O_3 which do not vary the crystalline phase of CeO_2–ZrO_2 solid solution but distort the crystal lattice obviously. They are the most effective additives for improving the surface area, thermal stability, and reducibility of CeO_2–ZrO_2, and they can also promote the catalytic activity of Pd/CeO_2–ZrO_2 for methane combustion. The second group includes La_2O_3, Pr_2O_3, and Nd_2O_3, which can also keep the same crystalline phase, distort the crystal lattice, and improve the surface area and thermal stability of the solid solution, but their effects are much weaker and they decrease the reducibility of the solid solution. The third group includes BaO and CuO, whose effects on the property of CeO_2–ZrO_2 are much different. BaO and CuO, especially CuO, can decrease the thermal stability, and reduction extent of CeO_2–ZrO_2. CuO-modified CeO_2–ZrO_2 calcined at 550 °C shows the comparable high activity for the methane combustion, but after being calcined at 900 °C, CuO-modified CeO_2–ZrO_2 would separate into three phases as CeO_2, ZrO_2, and CuO, resulting in the much lower activity for the methane catalytic combustion.

X. Wang · G. Lu (✉) · Y. Guo · L. Jiang · Y. Guo
Lab for Advanced Materials, Research Institute of Industrial Catalysis, East China University of Science and Technology, Shanghai 200237, People's Republic of China
e-mail: gzhlu@ecust.edu.cn

X. Wang · C. Li
Key Laboratory for Ultrafine Materials of Ministry of Education, East China University of Science and Technology, Shanghai 200237, People's Republic of China
e-mail: 1111wangxh@163.com

Introduction

CeO_2 is an important component of three-way catalyst (TWC) due to its well-known promotion to the catalysts. It can act as "oxygen buffer" to undergo effective reduction/oxidation cycles by a reversible transition between CeO_2 and Ce_2O_3 with very different oxygen stoichiometries [1]. It can also stabilize the dispersion of precious metals and the structure of alumina support [2], promote the water–gas shift and the steam-reforming reactions [3], and suppress the strong interaction between the precious metals and alumina [4]. However, pure ceria would sinter easily at high temperature, thus resulting in the degeneration of its property. For this reason, CeO_2–ZrO_2 solid solution has been developed and used widely in TWC since the mid-1990s. As an important promoter in TWC, CeO_2–ZrO_2 solid solution should possess a single-phase structure, high thermal stability, and redox property, and so on. The pivotal properties of CeO_2–ZrO_2 can be obtained by using suitable preparation method and additives [5–9]. For example, Schulz et al. [5] proved that the addition of suitable amount of silica improves the oxygen exchange capacity of CeO_2–ZrO_2 solid solution. Fernández-García et al. [6] reported that the addition of Ca into the ceria–zirconia oxidic network could strongly modify its surface and bulk oxygen-handling property. Wang et al. [8] found that small amount of Pr favors the conversion of C_3H_6 and

NO on CeO_2–ZrO_2 solid solution. Although the effects of some additives on certain property of CeO_2–ZrO_2 solid solution have been investigated and reported, a systematic and regular investigation has been hardly reported. In other words, as the preparation methods used by different researchers are different, a general law for the effect of different additives exerted on CeO_2–ZrO_2 solid solution cannot be drawn simply, and how to choose the right additive to get the CeO_2–ZrO_2 solid solution with specific property still remains unclear.

The primary objective of this study is to get a clear picture about the effects of some typical oxides exerted on CeO_2–ZrO_2 solid solution. Therefore, the oxides chosen as the additives of CeO_2–ZrO_2 solid solution should be obviously representative and can represent almost all the properties of the oxides on the Periodic Table of Elements. Ba, Al, Cu, and Si were chosen as the representatives of the alkaline earth metals, the third main group metals, the transition metals, and the fourth main group elements. Nd, Pr, and La were chosen as the representatives of the rare earth elements. The choice of the additives are based on the following reasons: First, the reduction of Ce^{4+} (radius = 0.097 nm) to Ce^{3+} (0.114 nm) can lead to an expansion of lattice volume of CeO_2–ZrO_2, which may make this reduction more difficult. This negative effect would be decreased by an insertion of the cation with smaller ionic radius near Ce^{4+}, and then it accelerates the valence change between Ce^{4+} and Ce^{3+}. Based on this reason, SiO_2 (Si^{4+} radius = 0.026 nm) and Al_2O_3 (Al^{3+} radius = 0.054 nm) were used as the additives. Second, an incorporation of cationic additives with a lower oxidation state than +IV into CeO_2 lattice leads typically to formation of intrinsic oxygen vacancies, which helps to release stress caused by the cation size mismatch. This is a main reason to choose BaO (Ba^{2+}) as the dopant. Third, BaO, SiO_2, and La_2O_3 are usually used for improving the thermal stability of the metal oxides such as Al_2O_3, CuO, and Pr_2O_3 as a kind of oxygen storage material, and La, Pr, and Nd possess the similar electronic structure and property as that of Ce.

Summarizing the considerations above, M_yO_x (M = Al, Ba, Cu, La, Nd, Pr, Si)-modified CeO_2–ZrO_2 solid solutions have been prepared by a reverse microemulsion method, and their surface area, crystalline phase structure and reducibility were investigated by N_2 adsorption, using X-ray diffraction (XRD), FT-IR, ^{29}Si MAS NMR and Temperature Programmed Reduction (TPR).

Furthermore, the interest in the study on the methane catalytic combustion arises due to two reasons: the pollution abatement and power generation. An ideal catalyst for high temperature combustion of methane should possess high thermal stability as well as high catalytic activity. However, these two characteristics in the same catalyst seldom go hand in hand. Generally speaking, the noble metal catalysts (such as Pd or Pt) have high catalytic activity but low thermal stability, while the metal oxide catalysts have high thermal stability but low catalytic activity [10]. The study of Zhang et al. [11] showed that, ceria with high reducibility and oxygen storage capacity make it an extremely important component in the combustion catalyst. Zamar et al. [12] proved that the addition of ZrO_2 into CeO_2 leads to the formation of CeO_2–ZrO_2 solid solution with defective structure, which is favorable to the combustion of methane. So the methane combustion was used as a model reaction to investigate the catalytic performance of M_yO_x-modified CeO_2–ZrO_2 solid solution in this article.

Experimental

M_yO_x (M = Al, Ba, Cu, La, Nd, Pr, Si)-modified CeO_2–ZrO_2 (Ce/Zr = 1:1) solid solutions were prepared by a reverse microemulsion method as follows: (1) The mixture aqueous solution of cerium nitrate and zirconium nitrate and other metal nitrate or ethyl silicate was mixed with the mixture solution of polyethylene glycol octylphenyl ether (as surfactant), cyclohexane (as oil phase) and 1-hexanol (as co-surfactant) to obtain the reverse microemulsion of the salts (water/surfactant/cosurfactant/oil phase = 1.5/1/1.2/7.2, v/v/v/v). (2) Ammonia reverse microemulsion was obtained by mixing ammonia with the mixture of polyethylene glycol octylphenyl ether, cyclohexane, and 1-hexanol (water/surfactant/cosurfactant/oil phase = 1.5/1/1.2/7.2, v/v/v/v). (3) The salts and ammonia reverse microemulsions were mixed in a flask to react. All the experiments above are performed at room temperature. The precipitate was filtered, dried at 100 °C for 12 h, and then calcined at 550 °C for 5 h (or 900 °C for 6 h). The samples prepared were denoted as Ce–Zr–M–O (M = Al, Ba, Cu, La, Si, Nd, or Pr and its concentration was about 5.2 wt%).

Supported Pd catalyst was prepared by the wet impregnation of Ce–Zr–O–M support (20–40 mesh) with H_2PdCl_4 aqueous solution. The impregnated samples were dried in vacuum, and then calcined at 550 °C for 5 h in air. The Pd loading is 0.2 wt%.

The BET surface area and pore diameter distribution of the samples were measured at −196 °C with nitrogen as an adsorbent on a ST-03 type instrument of surface area and pore diameter distribution (Beijing Analytic Instrument Plant). The X-ray diffraction (XRD) patterns of the samples were recorded on a Rigaku D/max-2550/PC diffractometer operated at 50 KV and 180 mA, with CuKα radiation (λ = 1.54056 Å). Average particle sizes were estimated by the X-ray diffraction peaks with broadening and Scherrer equation of $\beta = K\lambda/Lw \cdot \cos\theta$, where K is a constant and taken as 1 here, λ is the X-ray wavelength, and β is the corrected peak width. The distortion rate of crystal lattice

(e) was estimated by the equation of $e = 1/4\ \beta \cdot ctg\ \theta$, where β is the corrected peak width. The solid-state ^{29}Si MAS NMR spectra were recorded on a Bruker AVANCE-500 spectrometer at 99.4 MHz, using 4-mm zirconium oxide rotor, a rotation frequency of 4,000 Hz, and tetramethyl silane as an external standard. The FT-IR spectra of the samples were recorded on a Nicolet Nexus 670 FT-IR spectrometer, and the sample to be measured was ground with KBr and pressed into a thin wafer.

Temperature-programmed reduction (TPR) of the samples was carried out in a conventional flow system equipped with a thermal conductivity detector (TCD). The sample was pretreated in N_2 at 500 °C for 1 h before TPR runs. The composition of reduction gas was 8% H_2/N_2 (25 mL min^{-1}) and the heating rate was 10 °C min^{-1}. The amount of hydrogen consumption of the sample was quantified by the integral of all the reduction peaks. TT was defined as the top temperature of the reduction peak, HC was defined as the amount of hydrogen consumption per molar cerium atom, OR was defined as the amount of oxygen release per molar cerium atom and RE was defined as the reduction extent (the ratio of $Ce^{3+}/(Ce^{4+} + Ce^{3+})$). OR and RE were derived from HC according to the reaction equation of $CeO_2 + H_2 = 1/2Ce_2O_3 + H_2O$.

The catalytic activity of the sample for the methane combustion was tested in the fixed bed with a quartz glass reactor packed 0.1 g catalyst. The reaction gas consisting of 2% CH_4, 8% O_2, and 90% N_2 (volume) was fed to the catalyst bed at GHSV of 48,000 h^{-1}. The reaction gas composition was analyzed on-line by GC with TCD detector.

Results and discussion

Textural property

Table 1 shows that when calcined at 550 °C for 5 h, the BET surface area of M_yO_x-modified CeO_2–ZrO_2 (M = Al, Ba, Cu, La, Nd, Pr, Si) is higher than that of single CeO_2–ZrO_2 solid solution. Among them, Ce–Zr–Si–O has the largest surface area (150 $m^2\ g^{-1}$). After being calcined at 900 °C for 6 h, the surface areas of all the samples decrease significantly. The sintering extent (SE, defined as surface area decrease fraction led by high temperature calcination) changes in the order of Ce–Zr–Si–O < Ce–Zr–Al–O = Ce–Zr–Nd–O < Ce–Zr–Pr–O < Ce–Zr–La–O < Ce–Zr–O < Ce–Zr–Ba–O < Ce–Zr–Cu–O. It indicates that Si, Al, Nd, Pr, and La not only increase the surface area of CeO_2–ZrO_2, but also inhibit its sintering. In other words, they can improve the thermal stability of CeO_2–ZO_2. Ce–Zr–Si–O has the highest thermal stability (SE = 49%), and its surface area can still maintain 76 $m^2\ g^{-1}$ even after being calcined at 900 °C for 6 h. Although Ba and Cu also increase the surface area of CeO_2–ZrO_2 calcined at 550 °C, they have no favorable effect on the improvement of its thermal stability, especially for Cu. It decreases the surface area of Ce–Zr–Cu–O to 6 $m^2\ g^{-1}$ when calcined at 900 °C for 6 h.

Table 1 The BET surface areas of the samples

Sample	BET surface area ($m^2\ g^{-1}$)		$\frac{S_{550}-S_{900}}{S_{550}}$ (%)[b]
	550 °C/5 h[a]	900 °C/6 h	
Ce–Zr–O	96	29	70
Ce–Zr–Ba–O	110	30	73
Ce–Zr–Cu–O	114	6	95
Ce–Zr–Al–O	118	53	55
Ce–Zr–Si–O	150	76	49
Ce–Zr–La–O	122	39	68
Ce–Zr–Pr–O	108	35	64
Ce–Zr–Nd–O	118	53	55

[a] The calcination condition

[b] The sintering extent

As a representative sample, Ce–Zr–Si–O was selected to investigate the effect of additives on the surface area and thermal stability of CeO_2–ZrO_2. When calcined at 900 °C for 6 h, the surface area of pure silica prepared by the same method is only 75 $m^2\ g^{-1}$, which is similar to that of Ce–Zr–Si–O (76 $m^2\ g^{-1}$), and that of single CeO_2–ZrO_2 is only 29 $m^2\ g^{-1}$. This means that the surface area of Ce–Zr–Si–O (5.2 wt% Si) is not the simple summation of the surface area of SiO_2 and CeO_2–ZrO_2. The enhancement of the surface area of Ce–Zr–Si–O after being calcined at high temperature is due to the synergistic reaction between SiO_2 and CeO_2–ZrO_2. In fact, SiO_2 is an effective additive not only for improving the surface area and thermal stability of CeO_2–ZrO_2, but also for that of other metal oxides such as alumina [13–15]. Figure 1 shows the pore diameter distribution curves of Ce–Zr–O and Ce–Zr–Si–O calcined at 900 °C for 6 h. The pore diameters of Ce–Zr–O and Ce–Zr–Si–O are 10–50 nm and 2–10 nm, respectively, which indicates that Si can inhibit the loss of meso-pores to retain its high surface area of CeO_2–ZrO_2 at high temperature.

Powder X-ray diffraction, FT-IR, and ^{29}Si MAS NMR

The XRD patterns of M_yO_x-modified CeO_2–ZrO_2 calcined at 550 °C are shown in Fig. 2. Although there is a little shift in peak position of different samples, they can still be ascribed to tetragonal $Ce_{0.5}Zr_{0.5}O_2$. This shift is indicative of change in lattice parameter, and it is evident that additives elements can insert into the solid solution [16]. With the addition of other additives, peak broadening is also observed, which is due to the formation of small crystallite

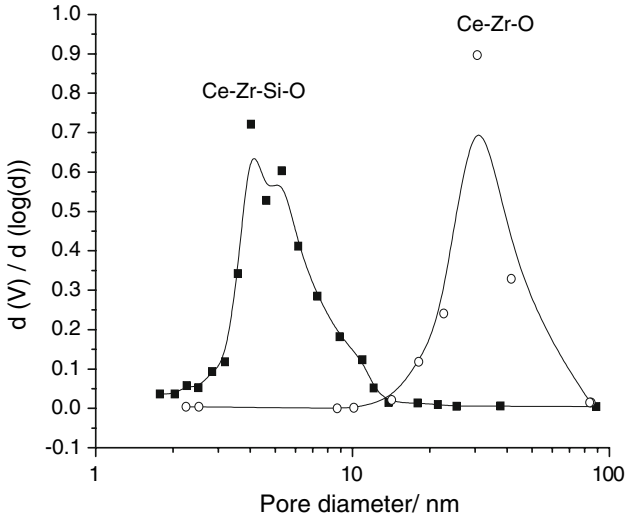

Fig. 1 Pore diameter distribution curves of Ce–Zr–O and Ce–Zr–Si–O calcined at 900 °C for 6 h

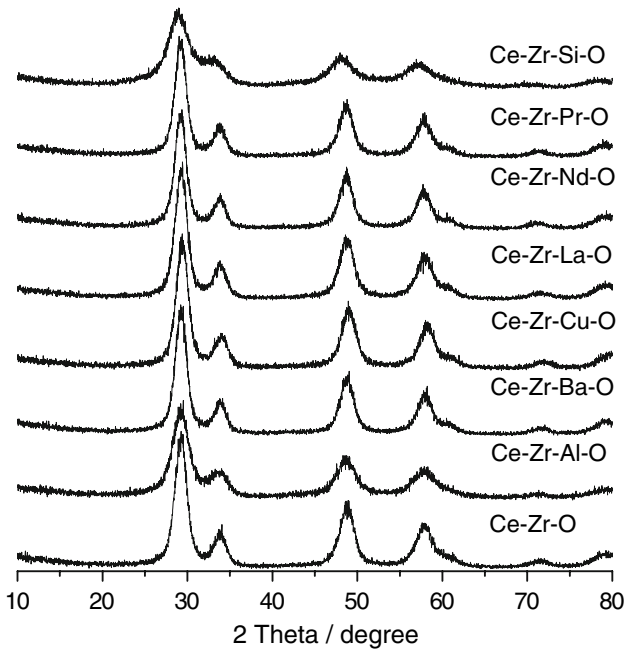

Fig. 2 XRD patterns of the samples calcined at 550 °C for 5 h

and much crystal lattice defect. Due to the high dispersion of the additives or their insertion into the solid solution, the diffraction peaks of the additives are not detected.

Compared with the XRD spectra (Fig. 2) of the samples calcined at 550 °C for 5 h, the diffraction peaks (Fig. 3) of all the samples calcined at 900 °C for 6 h become narrow, which reveals that the samples calcined at high temperature have the high crystallinity and larger crystallite. On the other hand, the XRD patterns of Ce–Zr–Cu–O calcined at 900 °C are much different from that of the sample calcined at 550 °C, and the diffraction peaks can be ascribed to

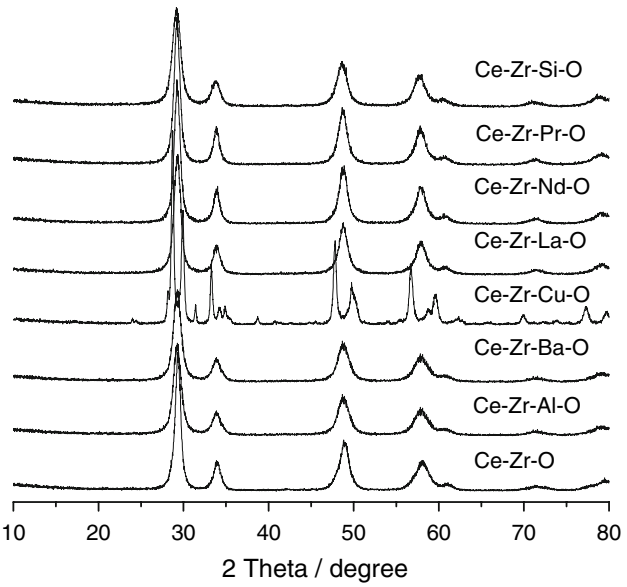

Fig. 3 XRD patterns of the samples calcined at 900 °C for 6 h

CeO_2, ZrO_2, and CuO, which indicates that Cu decreases the structural stability of CeO_2–ZrO_2. Combining with the results in Table 1, the noticeable loss of surface area of Ce–Zr–Cu–O at 900 °C is induced by the crystalline phase separation of the solid solution.

The crystallite sizes and crystal lattice distortion extent of the samples derived from the XRD patterns are shown in Table 2. The samples calcined at 550 °C for 5 h have the similar crystallite size of 10–11 nm. When calcined at 900 °C, their crystallite sizes increase due to the sintering. But all the modified CeO_2–ZrO_2 solid solutions (except Ce–Zr–Cu–O) have smaller crystallite than CeO_2–ZrO_2. It proves that M_yO_x (excluding CuO) can inhibit the growth of crystallite under heat treatment. Among them, Ce–Zr–Si–O has the smallest crystallite and the highest thermal stability,

Table 2 The crystallite sizes and crystal lattice distortion extent of the samples

Sample	Crystallite size (nm)		Crystal lattice distortion extent	
	550 °C/5 h[a]	900 °C/6 h	550 °C/5 h	900 °C/6 h
Ce–Zr–O	10	16	0.0139	0.0098
Ce–Zr–Al–O	10	13	0.0154	0.0122
Ce–Zr–Ba–O	11	15	0.0141	0.0096
Ce–Zr–Cu–O	11	33[b]	0.0141	0.0049[b]
Ce–Zr–La–O	11	14	0.0148	0.0110
Ce–Zr–Nd–O	11	15	0.0137	0.0101
Ce–Zr–Pr–O	11	15	0.0140	0.0102
Ce–Zr–Si–O	10	12	0.0156	0.0131

[a] The calcination condition

[b] The correlative data of ceria

which coincide with the results of BET surface area. The data of the crystal lattice distortion extent in Table 2 shows that, SiO_2 and Al_2O_3 distort the crystal lattice of the CeO_2–ZrO_2 solid solution obviously, and when calcined at high temperature, the promotion effect is noticeably more. Since the oxygen exchange capacity (OEC) of CeO_2–ZrO_2 is associated with its crystallinity and defects [5], the increase of crystal lattice distortion extent of Ce–Zr–Si–O and Ce–Zr–Al–O is favorable for the oxygen storage and release.

As SiO_2 is the most effective promoter to improve the surface area and thermal stability of CeO_2–ZrO_2 solid solution, Ce–Zr–Si–O has been chosen as a model to be characterized by FT-IR and ^{29}Si MAS NMR to clarify whether Si gets inserted into the crystal lattice of CeO_2–ZrO_2. As shown in Fig. 4, there are four absorption peaks near 1110, 1220, 804, and 464 cm^{-1} in the FT-IR spectrum of pure SiO_2 prepared by a reverse microemulsion method and calcined at 900 °C for 6 h. These features are related to strongly bonded Si–O–Si bridges in typical SiO_2 [17]. In the Ce–Zr–Si–O, the absorption peaks at 804 and 464 cm^{-1} disappeared and the peak at 1,110 cm^{-1} shifted to much lower band. This means that the Si–O–Si bridges of SiO_2 in the Ce–Zr–Si–O solid solution is changed. The reason may be the formation of Si–O–M (Ce or Zr) bridges in the Ce–Zr–Si–O solid solution, which indicates that Si can get inserted into the crystal lattice of CeO_2–ZrO_2.

^{29}Si NMR spectra of pure SiO_2 and Ce–Zr–Si–O calcined at 900 °C for 6 h are shown in Fig. 5. In the spectrum of pure SiO_2, the main peak at −110 ppm (chemical shifts) is ascribed to Q^4 that represents the silicon with $Si(OSi)_4$ [18, 19]. In the spectrum of Ce–Zr–Si–O, the peak around −106 ppm is predominant. This peak is also often observed in some M-MCM compounds such as Fe-MCM and Zr-HMS, and can be assigned to $Si(OSi)_3(OM)$ [20–22]. These results confirm the formation of the bridges of Si–O–M (M = Ce or Zr) bonds.

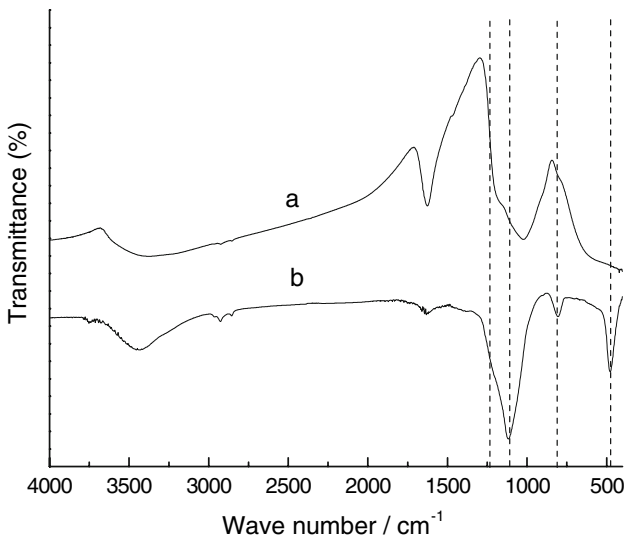

Fig. 4 FT-IR spectra of Ce–Zr–Si–O (**a**) and SiO_2 (**b**) calcined at 900 °C for 6 h

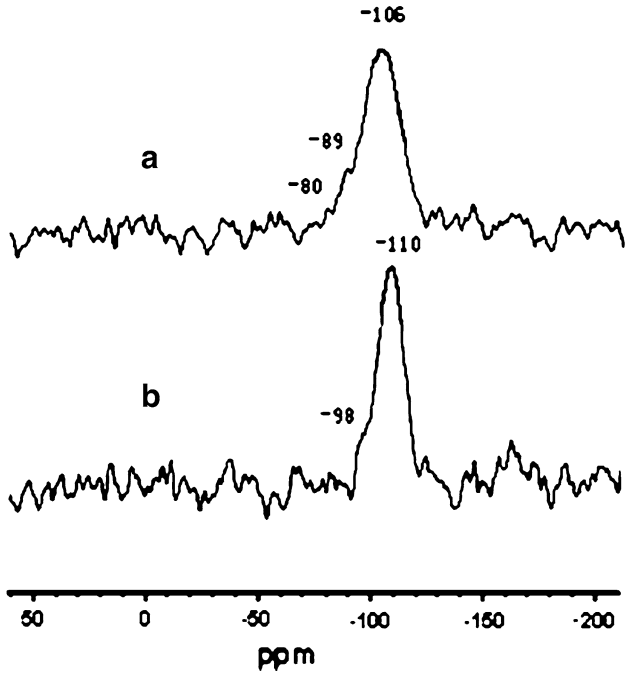

Fig. 5 ^{29}Si NMR spectra of Ce–Zr–Si–O (**a**) and pure SiO_2 (**b**) calcined at 900 °C for 6 h

H_2-TPR

TPR profiles of M_yO_x-modified CeO_2–ZrO_2 calcined at different temperature are shown in Figs. 6 and 7, and their reduction characteristic data derived from these profiles are listed in Table 3, which include the reduction extent (RE), amount of hydrogen consumption (HC), and oxygen release (OR). CeO_2–ZrO_2 calcined at 550 °C gives a very broad and asymmetric reduction peak at 280–660 °C, and the top temperature (TT) is about 564 °C, which can be ascribed to the reduction of Ce^{4+} (surface Ce^{4+} and bulk Ce^4). The reduction temperature of surface Ce^{4+} is generally at <400 °C, but it can not be distinguished clearly from the reduction of bulk Ce^{4+}.

Compared with the TPR profile of CeO_2–ZrO_2, the TT of the reduction peak of Ce–Zr–Al–O, Ce–Zr–Ba–O, and Ce–Zr–Si–O is lower. That is to say, some bulk Ce^{4+} in these samples can be reduced more easily. The improvement of the bulk reducibility of CeO_2–ZrO_2 may be correlated to the distortion of the oxygen sublattice, which increases the anionic mobility [23]. The starting reduction

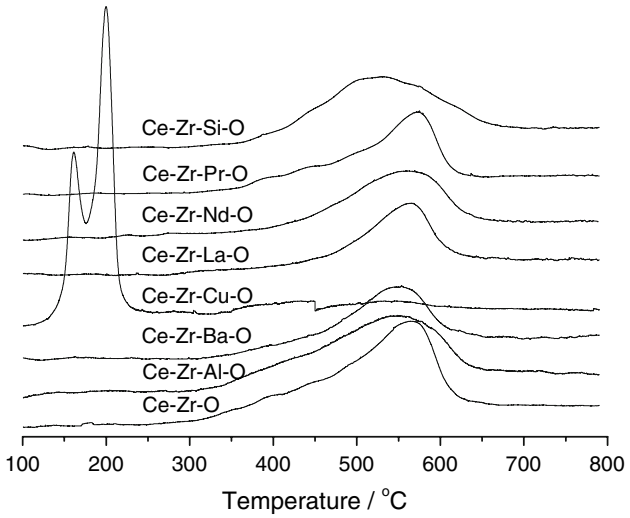

Fig. 6 TPR profiles of the samples calcined at 550 °C for 5 h

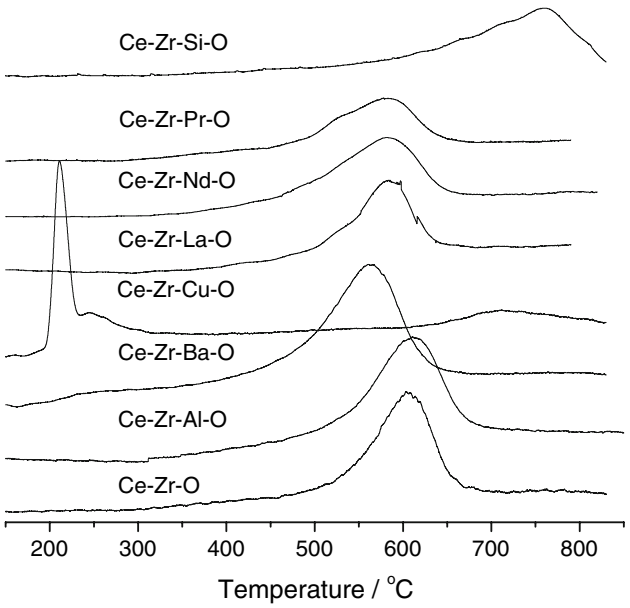

Fig. 7 TPR profiles of the samples calcined at 900 °C for 6 h

temperature of Ce–Zr–La–O, Ce–Zr–Pr–O and Ce–Zr–Nd–O rises, but the peak TT changes a little. Being different from other modified CeO_2–ZrO_2 samples, CuO modified Ce–Zr–O exhibits the completely different TPR profile, which is probably due to the easy reduction of CuO by H_2. In the TPR process of Ce–Zr–Cu–O, the reduction of CuO at low temperature can promote the reduction of Ce^{4+} at lower temperature through the interaction between CuO and CeO_2–ZrO_2 or the hydrogen spillover.

As high temperature calcination leads to the sintering, the loss of the surface area and crystal defects, which hinders the contact between hydrogen and sub-lattice oxygen and depresses the anionic mobility, the reduction peaks of the samples calcined at 900 °C for 6 h become narrow and shift to higher temperature. Like the reduction temperature, the RE is also an important reducibility parameter and is relative to the oxygen handling capacity. The results in Table 3 show that, Al and Si not only decrease the reduction temperature of the solid solution, but also increase its RE. When calcined at 550 °C, the RE of Ce–Zr–Si–O can reach 98% and it still holds 82% even after being calcined at 900 °C for 6 h. The HC and OR of Ce–Zr–Si–O calcined at 550 °C (900 °C) are 490 and 410 (245 and 215) mmol (mol Ce)$^{-1}$, respectively.

Activity for the methane catalytic combustion

The catalytic activities of M_yO_x-modified CeO_2–ZrO_2 are listed in Table 4. The results show that the catalytic activity of all Ce–Zr–M–O is higher than that of Ce–Zr–O except that of Ce–Zr–Al–O and Ce–Zr–Si–O. The catalytic activity of the samples decreases in the order of Ce–Zr–Cu–O > Ce–Zr–La–O > Ce–Zr–Ba–O > Ce–Zr–Nd–O > Ce–Zr–Pr–O = Ce–Zr–O > Ce–Zr–Al–O > Ce–Zr–Si–O. Although Al and Si can improve the thermal stability and reducibility of CeO_2–ZrO_2, they do not improve its methane catalytic combustion activity. However, Ce–Zr–Cu–O calcined at 550 °C exhibits the very high activity for the methane combustion, and its ignition temperature ($T_{50\%}$) is

Table 3 Reduction property of the samples

Sample	RE (%)		HC (mmol (mol Ce)$^{-1}$)		OR (mmol (mol Ce)$^{-1}$)	
	550 °C/5 h[a]	900 °C/6 h	550 °C/5 h	900 °C/6 h	550 °C/5 h	900 °C/6 h
Ce–Zr–O	75	70	375	350	188	175
Ce–Zr–Al–O	96	76	480	380	240	190
Ce–Zr–Ba–O	74	58	370	290	185	145
Ce–Zr–Cu–O	73	15	365	75	183	38
Ce–Zr–La–O	58	57	290	285	145	143
Ce–Zr–Nd–O	65	57	325	285	168	143
Ce–Zr–Pr–O	68	51	340	255	170	128
Ce–Zr–Si–O	98	82	490	410	245	215

[a] The calcination condition

Table 4 Methane catalytic combustion activity of the catalysts

Sample[a]	Calcined at 550 °C/5 h[b]			Calcined at 900 °C/6 h		
	$T_{10\%}$ (°C)	$T_{50\%}$ (°C)	$T_{90\%}$ (°C)	$T_{10\%}$ (°C)	$T_{50\%}$ (°C)	$T_{90\%}$ (°C)
Ce–Zr–Cu–O	377	465	530	558	690	770
Pd/Ce–Zr–Cu–O				510	650	750
Ce–Zr–La–O	427	500	580	480	580	660
Pd/Ce–Zr–La–O				430	520	580
Ce–Zr–Ba–O	430	520	590	500	575	645
Pd/Ce–Zr–Ba–O				380	530	620
Ce–Zr–Nd–O	450	530	600	470	570	640
Pd/Ce–Zr–Nd–O				410	530	590
Ce–Zr–Pr–O	460	530	580	462	556	628
Pd/Ce–Zr–Pr–O				310	530	610
Ce–Zr–O	460	530	620	510	598	665
Pd/Ce–Zr–O				430	560	650
Ce–Zr–Al–O	460	540	630	510	600	690
Pd/Ce–Zr–Al–O				360	490	590
Ce–Zr–Si–O	490	570	680	570	680	740
Pd/Ce–Zr–Si–O				360	430	540

[a] The loading of palladium was 0.2 wt% and the catalysts were calcined at 550 °C for 5 h

[b] The calcination condition of solid solution

only 465 °C, which can be comparable with many supported noble metal catalysts, such as the Pd catalyst supported on alumina doped with La or Sn [24].

After being calcined at 900 °C for 6 h, their methane catalytic combustion activities decrease obviously, which may be caused by the drastic loss in the surface area, growth in the crystallite, enhancement of crystallinity extent, and decrease of the oxygen handling property. The phase separation of Ce–Zr–Cu–O calcined at 900 °C makes the cooperation between CuO and CeO_2 lose, thus leading to the activity decrease remarkably.

The catalytic activities of the 0.2%Pd/Ce–Zr–M–O catalysts for the methane combustion are listed in Table 4. The results show that the activities of all the samples are increased by the promotion of 0.2 wt% Pd, especially for 0.2% Pd/Ce–Zr–Al–O and 0.2% Pd/Ce–Zr–Si–O. $T_{10\%}$, $T_{50\%}$, and $T_{90\%}$ of Pd/Ce–Zr–Si–O are 360, 430, and 540 °C, respectively, which is much lower than that of the other supported catalysts. The results above indicate that, Ce–Zr–Si–O and Ce–Zr–Al–O are the perfect supports of Pd catalyst for the methane catalytic combustion.

Conclusions

To summarize the effects of different additives on the structure characteristics, thermal stability, reducibility, and catalytic activity of CeO_2–ZrO_2 solid solution for methane combustion, it is concluded that SiO_2 and Al_2O_3 are the most effective additives for improving the surface area, thermal stability, and reducibility of CeO_2–ZrO_2 solid solution. La_2O_3, Nd_2O_3, and Pr_2O_3 can also improve the surface area and thermal stability of CeO_2–ZrO_2 to a limited extent, but weaken its reduction extent. BaO and CuO decrease the thermal stability and reduction extent of CeO_2–ZrO_2. When used as catalyst or catalyst support for methane combustion, Ce–Zr–Cu–O calcined at 550 °C for 5 h has the comparable high activity, but it is not a good kind of support of Pd catalyst. SiO_2 or Al_2O_3-modified CeO_2–ZrO_2 behaves with the lowest activity, but they are the excellent supports of Pd catalyst.

Acknowledgements This study was supported financially by the National Basic Research Program of China (2004CB719500), the National Natural Science Foundation of China (20601008), the Commission of Science and Technology of Shanghai Municipality (05QMX1415, 0452nm005), and Rare Earths Office of Shanghai Municipality (200503).

References

1. Ozawa M (1998) J Alloy Compd 275–277:886
2. Gandhi HS, Shelef M (1987) Stud Surf Sci Catal 30:199
3. Kim G (1982) Ind Eng Chem Pro Res Dev 21:267
4. Suhonen S, Valden M, Hietikko M, Laitinen R, Savimäki A, Härkönen M (2001) Appl Catal A Gen 218:151
5. Schulz H, Stark WJ, Maciejewski M, Pratsinis SE, Baiker A (2003) J Mater Chem 13:2979
6. Fernández-García M, Martínez-Arias A, Guerrero-Ruiz A, Conesa JC, Soria J (2002) J Catal 211:326
7. Chen M, Zhang P, Zheng X (2004) Catal Today 93–95:671
8. Wang W, Lin P, Fu Y, Cao G (2002) Catal Lett 82:19
9. Ikryannikova LN, Markaryan GL, Kaharlanov AN, Lunia EV (2003) Appl Surf Sci 207:100
10. Choudhary TV, Banerjee S, Choudhary VR (2002) Appl Catal A Gen 234:1
11. Zhang Y, Andersson S, Muhammed M (1995) Appl Catal B Environ 6:325

12. Zamar F, Trovarelli A, Deleitenburg C, Dolcetti G (1995) J Chem Soc Chem Commun 9:965
13. Wang X, Lu G, Guo Y, Wang Y, Guo Y (2005) Mater Chem Phys 90:225
14. Horiuchi T, Chen L, Osaki T, Sugiyama T, Suzuki K, Mori T (1999) Catal Lett 58:89
15. Horiuchi T, Osaki T, Sujiyama T, Suzuki K, Mori T (2001) J Non-Crystal Solids 291:187
16. Hori CE, Permana H, Simon Ng KY, Brenner A, More K, Rahmoeller KM, Belton D (1998) Appl Catal B 16:105
17. Campostrinil R, Ischial M, Armelao L (2004) J Therm Anal Calorim 78:657
18. Wiench JW, Avadhut YS, Maity N, Bhaduri S, Lahiri GK, Pruski M, Ganapathy S (2007) J Phys Chem B 111:3877
19. Sales JAA, Petrucelli GC, Oliveira FJVE, Airoldi C (2007) J Colloid Interface Sci 315:426
20. Hu LH, Ji SF, Xiao TC, Guo CX, Wu PY, Nie PY (2007) J Phys Chem B 111:3599
21. Choy JH, Yoon JB, Jung H, Park JH (2004) J Porous Mater 11:123
22. Yuan Z, Liu S, Chen T, Wang J, Li H (1995) J Chem Soc Commun 9:973
23. Vlaic G, Fornasiero P, Geremia S, Kaspar J, Graziani M (1997) J Catal 168:386
24. Fraga MA, Soares de Souza E, Villain F, Appel LG (2004) Appl Catal A Gen 259:57